

Multi-technical study of retrogressive thaw slumps at km 1456 of the Alaska Highway, Yukon

Fabrice Calmels, Philip Sedore, Fanny Amyot, Louis-Philippe Roy, Cyrielle Laurent, Casey Buchanan & Cathy Koot

YukonU Research Centre, Yukon University, Whitehorse, Yukon, Canada



ABSTRACT

The presence of active retrogressive thaw slumps (RTSs) adjacent to the Alaska Highway at km 1456 have created a unique opportunity for permafrost characterization, monitoring, and climate change impact analysis in the greater Whitehorse area. An intensive research program was established to act before serious damage occurs and acquire a better understanding of retrogressive thaw slumps that impact northern road corridors. The study addresses key knowledge gaps in mapping of RTS formation and evolution processes, as well as methodological gaps in the monitoring of such geohazards. To acquire this new knowledge about RTS processes, the study focuses on frozen soil properties, ground thermal regime, ground movements, and ground water dynamics. Research activities included geotechnical borehole investigations, ground temperature monitoring, ground surface movement monitoring with differential GPS, imaging and topography monitoring using unmanned aerial vehicle photogrammetry, and electrical resistivity tomography surveying. The multi-technical monitoring approach was used to inform an approach to mitigate the threat caused by RTSs on road corridors.

1 INTRODUCTION

Retrogressive thaw slumps (RTSs) occur in areas of ice-rich permafrost. They develop on hillslopes and usually occur along the shorelines of lakes, rivers and coastlines (Ramage et al. 2017). Thaw slumps consist of a headwall made predominantly of ice and a muddy slump floor. Slumps grow as melting ground ice in the headwall turns material into a muddy slurry that flows downslope to the base of the exposure (Kokelj and Jorgenson 2013; Armstrong et al. 2018; Ballantyne 2018). Melting of the exposed ground ice causes the headwall to retreat upslope and the disturbance grows. A headwall may migrate by several metres in a single summer, and over time a slump can impact several hectares of terrain. The rate of headwall movement is linked to several environmental factors, but generally, rates of slump growth are most rapid when the temperature is warmest (Bernard et al. 2021). Retrogressive thaw slump activity has increased in the Arctic in recent decades (Ward Jones et al. 2019; Lewkowicz and Way 2017), and their occurrence is projected to intensify in magnitude and frequency with a changing climate (Turner et al. 2021).

Retrogressive thaw slumps can represent permafrost thaw-related geohazards that may lead to widespread damage or lead to failure of northern transportation infrastructure. The development of some of these geohazards can be attributed to the thermal disturbances induced by the construction and presence of the very infrastructures themselves (Bliss and Ross 1971). Other thaw processes that are occurring naturally or as a function of climate change in the vicinity of infrastructures, sometimes even hundreds of meters away, can eventually impact them. Such an occurrence was reported along the Dempster Highway on the Peel Plateau (Kokelj et al. 2021; van de Suijs et al. 2018).

Two retrogressive thaw slumps formed close to the Alaska Highway at km 1456, approximately 30 km west of Whitehorse (Figure 1). They are located within a forested area surrounded by the Takhini River to the north and the

Alaska Highway to the south. The first RTS (RTS 1) was discovered in April 2019, while the second (RTS 2) initiated in September 2021.

The headwall of RTS 1 was approximately 80 m away from the road in May 2019. Given the RTS proximity to the Alaska Highway and the risk posed to road safety, a multi-technical study and monitoring program were implemented to address this hazard and provide the Transportation Engineering Branch of Yukon Highway and Public Works department with the information needed to address the issue. The study also provided the opportunity to investigate RTS formation and evolution processes in sporadic discontinuous permafrost zones.

This paper presents and discusses results obtained using a methodological approach combining Unmanned Aerial Vehicle (UAV) surveys, borehole geotechnical and temperature data, and electrical resistivity tomography (ERT) geophysical surveys that were used to develop a better understanding of the RTS processes in the area.

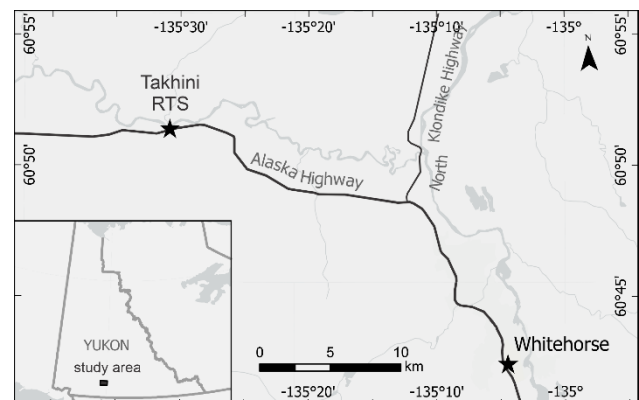


Figure 1. Study area map.

2 STUDY SITE

This section of the Alaska Highway is in the Southern Lakes Ecoregion (Yukon Ecoregions Working Group 2004). The

climate is subarctic with large seasonal variations in temperature and a mean annual air temperature (MAAT) of $-3.0\text{ }^{\circ}\text{C}$, which is $2.3\text{ }^{\circ}\text{C}$ cooler than the Whitehorse airport (Burn 1998). This area is also characterized by low precipitation and low humidity due to the rain shadow of the Coast Mountains. The site is covered by a deciduous mixed forest consisting of lodgepole pine, white spruce, and trembling aspen. Shrubs such as willow and soapberry are present throughout much of the site. Common plant species are forbs such as fireweed and alpine sweet-vetch, mosses, and lichens. The site lacks a thick organic cover.

The surficial geology and landscape features of the study site are largely a product of the most recent (Late Wisconsinan) McConnell Glaciation, which occurred between 24,000 and 11,000 years ago. At this location in the Ibex Valley, Glacial Lake Champagne deposited up to 75 m of silt and clay between 10,000 and 9,000 years ago (Yukon Ecoregions Working Group 2004). After the drainage of the lake, permafrost was able to aggrade in this sediment. In the Ibex Valley, glaciolacustrine silt and clay often contains massive ice bodies, which are prone to RTSs and general thermokarst degradation when disturbed by river erosion, forest fires, or other changes in surface conditions (H.M. French 2017).

The Takhini River RTSs were likely initiated by erosion on the outer bend of a meander of the Takhini River. Though studies began at this site in the spring of 2019, satellite and aerial imagery show the RTS 1 to have been active since at least 2014. The RTS 2 initiated in September 2021, during the monitoring program.

A similar failure had already occurred only 180 m east of this site. Aerial photography revealed that a $40,000\text{ m}^3$ RTS was initiated in 1979 by river bank erosion and stayed active until 1986, causing 112 m of headwall retreat to approximately its present position. Since 2004, that thaw slump stabilized a few meters short of the highway.

The study site is in sporadic discontinuous permafrost zone (Hegginbottom et al. 1995). Research led by Burn (1987, 1998) in a nearby forested site found a 1.4 m thick active layer, and 17 m thick permafrost, the temperature at the top of permafrost (TTOP) being $-0.7\text{ }^{\circ}\text{C}$. When the site RTS 1 was first assessed in May 2019, the then 50 m wide and 5 m high headwall provided an outstanding natural exposure of ice-rich permafrost with ice lenses that were up to 20 cm thick. The other noticeable signs of permafrost degradation on the study site were meter-wide tension cracks and split trees due to ground movements. Along the road in the cleared area, some shallow ponds are present, which probably have thermokarstic origins. A noticeable feature is groundwater that frequently seeps from the headwall of the slump during the thaw season and icings in winter.

3 METHODOLOGY

3.1 Below surface investigations

A total of four boreholes of various depths were drilled at the site (locations shown in Figure 2). Borehole 1 (BH1) and 2 (BH2) were drilled by a contractor using a CRREL corer

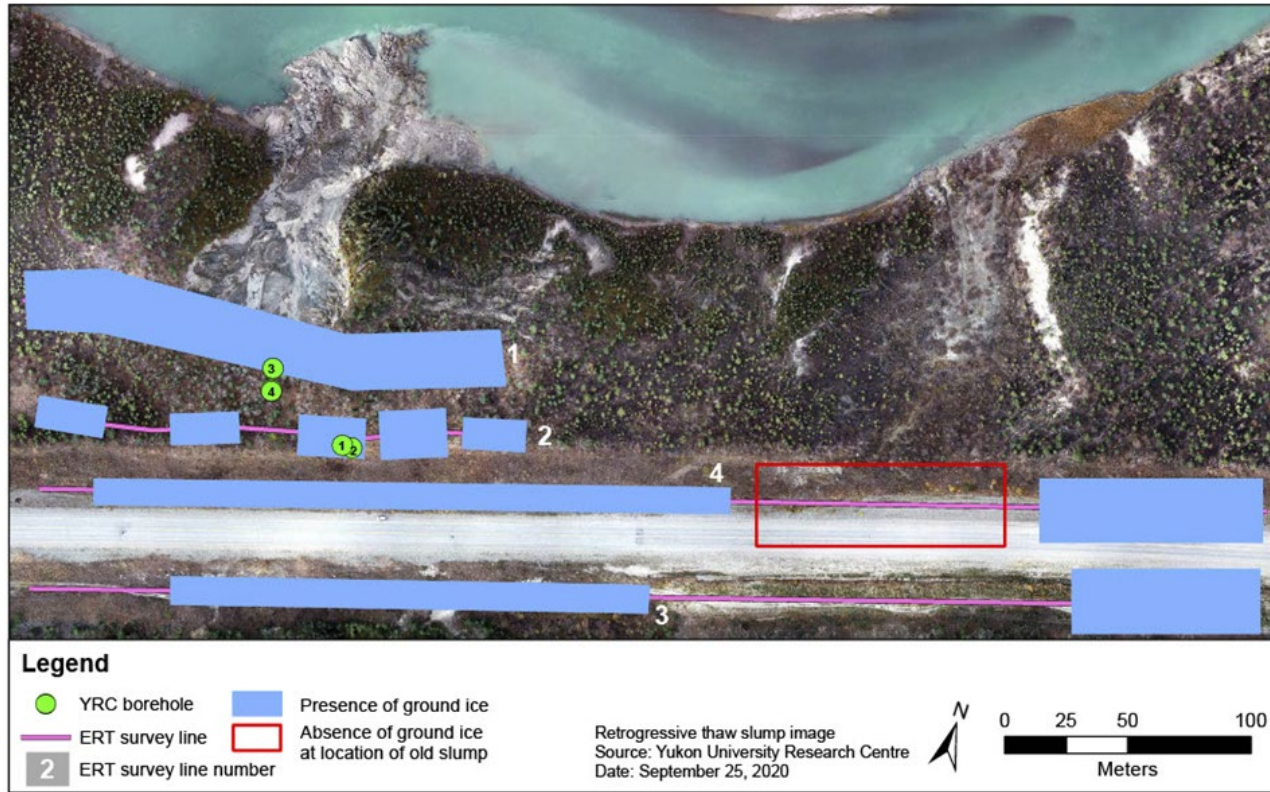


Figure 2. Boreholes and ERT line locations, with approximate position of ground ice based on ERT profiles.

for BH1 and destructively for BH2 on October 16 and 23, 2019, reaching 10 m and 25 m depths respectively.

Two shallow boreholes, BH3 and BH4, were drilled May 13 and May 22, 2020, by the research team with a portable core-drill system using a diamond-carbide corer, reaching 6 m and 3 m depth, respectively. Once drilling was completed, the boreholes were cased with 1-inch PVC conduits and backfilled to the surface. Groundwater was encountered at approximately 3 m depth in boreholes BH1, BH2, and BH4. It resulted in the collapsing of BH1 and BH4, and the termination of drilling.

Cores from BH1 and BH3 were brought frozen to the laboratory where grain-size, cryostructures, volumetric ice content, gravimetric ice content and settlement potential were analysed. A log for each permafrost borehole was then created. BH2 was outfitted with a 16-channel LogR Systems thermistor and logger, and BH3 with two 4-channel Hobo UX120 loggers to record ground temperatures. The two boreholes also were outfitted with MeasureAnd SAAV Shape Array inclinometer to monitor deformation and slope movements every 50 cm from the surface to the base.

Electrical resistivity surveys were performed using an ABEM Terrameter LS electrical resistivity and tomography system. Two 200 m ERT lines, profiles 1 and 2, were surveyed in the forested slump area using Wenner and dipole-dipole arrays with 2.5 m spacing between electrodes. Two 500 m ERT lines, profiles 3 and 4, were surveyed on each side of the road, at the base of the embankment, using a dipole-dipole array with 2.5 m spacing between electrodes (Figure 2). ERT 1 survey was completed on June 14, 2019. It ran from east to west, through a dense undisturbed deciduous mixed forest 12 m away from the RTS 1 headwall. ERT 2 was conducted on July 16, 2019. This transect ran east to west in a deciduous mixed forest, along the cleared portion of the right-of-way of the Alaska Highway and 30 m away from the RTS 1 headwall. ERT 3 was completed on August 23, 2019. The 500 m survey ran west-east along the south side of the road embankment, going down a slight hill slope. The vegetation cover was open and colonized predominantly by small trembling aspen, willows, and some spruce saplings. ERT 4 was completed on September 12, 2019. The 500 m survey ran west-east along the north side of the road embankment, going down a slight hill slope. The vegetation cover was very similar to that encountered at ERT 3.

3.2 Above surface investigations

The thaw slump has been regularly surveyed with drones for aerial image collection since August 2019 during thaw seasons. A DJI Phantom 4 Pro V2 was used from August 2019 to July 2020 and DJI Matrice RTK 210 from August 2020 until present. Targets were placed on the ground with their position geolocated using a differential global positioning system (DGPS). The targets' locations were used as ground control points to produce centimeter-scale positional accuracy for the image processing outcome products.

Images were processed using Agisoft Metashape Professional software. Image processing produced a point

cloud, a 3D model including mesh mapping and texture, a digital surface model (DSM), and an orthomosaic. All final products are projected using UTM zone 8. Orthomosaics and DSMs were used to digitize the headwall of the thaw slump with ArcGIS to measure the progression of the slump through a suite of morphometric parameters.

The groundwater seeping from the headwall of the slump was investigated and mapped flying a DJI Mavic 2 Enterprise Advanced Thermal November 21, 2021.

4 RESULTS

4.1 Borehole data

The cores of BH1 (Figure 3) shows a stratigraphy composed predominantly by clayey silt. The borehole ends at 10 m in silty sediment (99.9% silt). Lenticular, micro lenticular, reticulate and thick suspended cryostructures were identified along the profile. The volumetric excess ice content ranged from 13 to 41%. The horizon from 4.5 to 10 m contained the highest excess ice content. Overall, the borehole has a mean volumetric excess ice content of 32.5%.

The borehole BH3 shows layers of ice-rich gray clayey silt alternating with some very ice rich layers. While drilling was initiated in frozen ground, at approximately two meters depth a thin unfrozen section of soil with the presence of ground water depth was encountered. The borehole extends to six meters with clayey-silt sediment. Lenticular and micro lenticular cryostructures were identified along the profile.

Ground temperature records suggest that the top of permafrost is between two and three meters. The ground temperatures are just below 0 °C. The ground appears to be unfrozen below eight meters of depth in BH2 but cores were recovered frozen down to 10 m depth in BH1. This suggests that destructive drilling altered the thermal regime in BH2 and depth of permafrost cannot be inferred from the BH2 temperature record. The permafrost at this site can be considered as warm and susceptible to degradation. The significant amount of ice present in the ground is preventing permafrost from thawing because of the latent heat (the amount of heat required to melt all the ice in a unit of soil or rock) absorption required to change ice to liquid water.

4.2 ERT survey results

The ERT 1 survey (Figure 4) suggests that permafrost could be as deep as 30 m towards the eastern part of the survey, and at its shallowest towards the western end. Several high resistivity pockets, or clusters (darker blue shades), are present along the survey. Some lower resistivity cores (red shades) are present (~40 m). This could indicate the presence of underground water flow within the permafrost, due to the discontinuous distribution of permafrost in the Takhini Valley.

The ERT 2 (Figure 4) suggests that the permafrost is more discontinuous as we get closer to the highway. Similar high resistivity clusters (blue shades) to those observed in ERT 1 survey likely represent ice-rich permafrost. Permafrost distribution seems more localized and does not tend to go

deeper than 20 m at its deepest point (77.5 m along the profile). Low resistivity areas (red/orange shades) may indicate ice-poor and/or unfrozen material, or the presence of liquid ground water circulating within permafrost.



Figure 2. Ice-rich permafrost showing thick layered (top) and suspended (base) cryostructures in a core from BH1 at a depth of 657 cm.

The ERT 3 survey data (Figure 4) suggests a localized high resistivity area (dark blue) up to 7 m deep. Some deep, low resistivity pockets (red shades), visible at various locations, could be associated with groundwater flow.

The ERT 4 survey (Figure 4) also shows high resistivity area down to 7 m deep, along most of the profile. One large, highly resistive cluster, towards the east end of the profile shows potential ice-rich material from 17 to 35 m depth. Some shallow low resistivity pockets, between 5 and 10 m depth along the profile, could be associated with water flowing within permafrost.

Overall, the very high-resistivity areas (dark blue) are attributable to ice-rich fine-grained sediment (clayey-silts); they increase closer to the headwall and become more sporadic closer to the highway. The low resistivity values could be attributable to ice-poor and/or unfrozen material,

with the lowest values possibly indicating the presence of liquid ground water. Permafrost may also be present in areas with resistivity as low as 100 ohm.m, due to higher liquid water content in fine-grained material near 0 °C.

4.3 UAV surveys

Monthly surveys include high resolution UAV surveys as well as benchmark surveys using differential GPS. With these tools, combined with satellite imagery and LiDAR data from as early as September 2016, it has been possible to monitor the retreat of the RTS headwall since 2016. The retreat of the RTS headwalls from September 2016 to September 2023 is presented in Figure 5. The shortest distance from the headwalls to the road (DTR) and the surface areas (A) of the RTS were measured from each survey. The annual area growth percentage (AAG%) between two UAV survey years was calculated as well as the elongation (length/width) of the two RTSs. The results are presented in Table 1.

The RTS 1 headwall approached the highway at an average rate of 13 m/yr from 2016 to 2018, then experienced an ablation of 16 m in summer 2019, 13 m in summer 2020, 17 m in summer 2021, 3 m in summer 2022, and 1 m in summer 2023. The retreat of the headwall decreases in proximity of the right-of-way at the location of its central axis, while the headwall continues to widen along the east side, by 14 m in summer 2022 and 13 m in summer 2023. The headwall has shown minimal progression along at the west side during summer 2023. It must be noted that the central axis area has been disturbed by heavy machinery compacting the ground during an unsuccessful attempt by contractors to drill the waste area during winter 2022. This disturbance may have impacted the advance of the headwall at this location.

The RTS 2 started to be noticeable in October 2021. Its headwall was then 95 m from the road. It then advanced by 15 m in summer 2022 and 11 m in summer 2023, having a similar average of 13 m/yr to RTS 1 from 2016 to 2018.

The evolution of the elongation at RTS 1 show the slump is progressively rounding off, becoming as wide as it is long. Interestingly, after their first two years, RTS 1 and RTS 2, share the same elongation values in 2016 and 2023, respectively.

Since 2016, the RTS 1 AAG% decreases from a year to another, except for 2021. The AAG% of RTS 2 has increased over the first two years, with the surface area increasing more than twofold.

The thermal imagery survey performed in November 2021 was used to identify and locate more than a dozen groundwater springs flowing from the headwall at RTS 1 (red spots along headwall in Figure 6). No groundwater springs were visible along RTS 2 headwalls.

To investigate how air temperature and precipitation may impact the growth of RTS 1, the surface area growth percentages between two UAV surveys were compared to the thaw degree day value and the cumulative precipitation for the same duration.

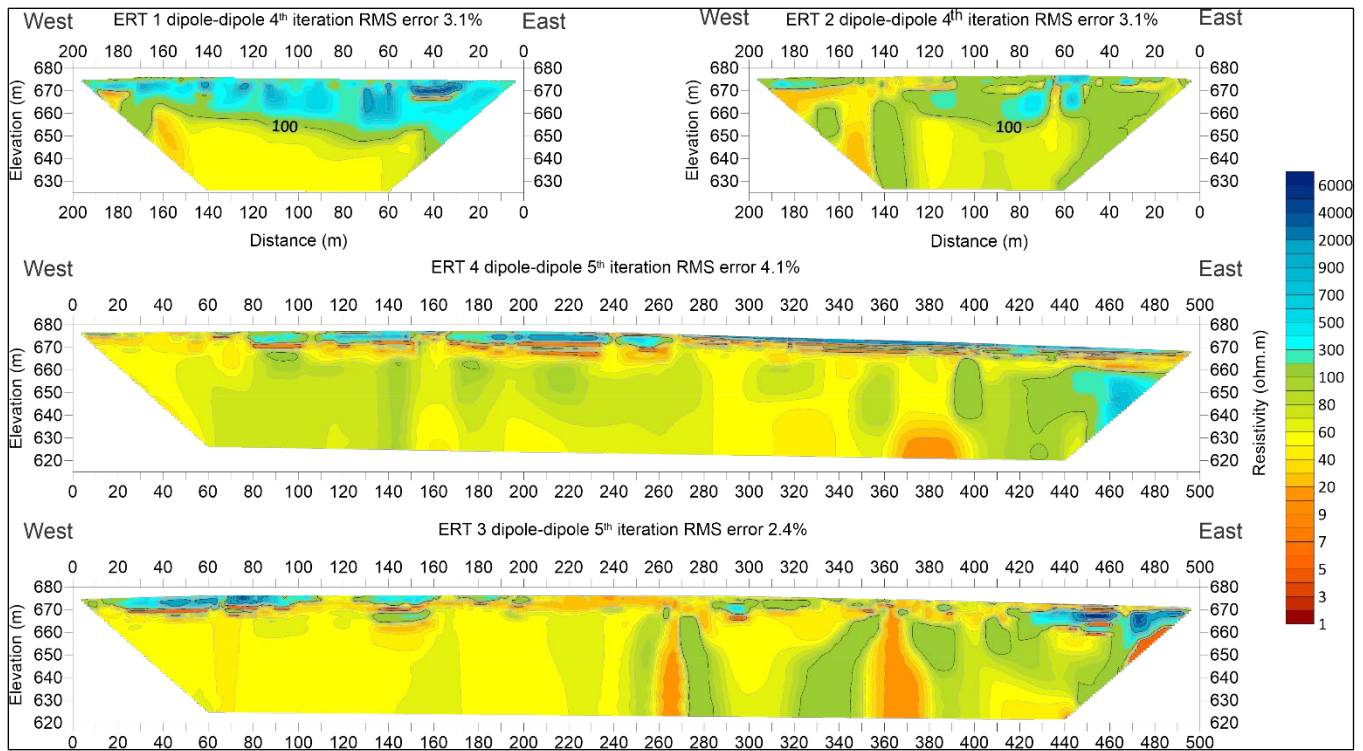


Figure 3. Four ERT profiles surveyed at the Takhini RTS site.

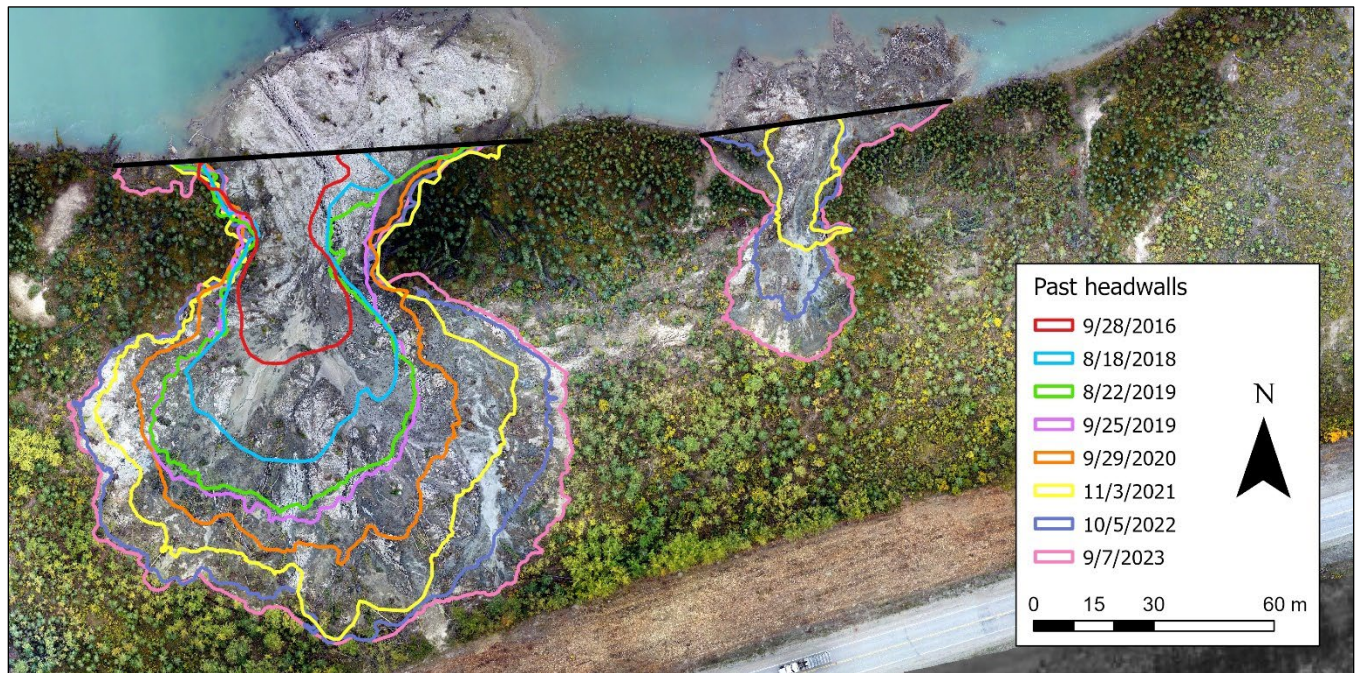


Figure 4. Retreat of the RTS headwalls from September 2016 to September 2023

Air temperature seems to have an influence on the area growth in 2020 ($R^2 = 0.9685$, $p = 0.0118$), 2021 ($R^2 = 0.6665$, $p = 0.0034$) and 2023 ($R^2 = 0.6403$, $p = 0.0014$), but not in 2022 ($R^2 = 0.1269$, $p = 0.0404$). Precipitation does not seem to have had an influence on the area growth except for 2022 ($R^2 = 0.8084$, $p = 0.0038$). The

2022 precipitation correlation likely is an anomaly as the slope of the regression line implies that higher precipitation slows down the RTS growth for this specific year, which contradicts basic permafrost thermodynamics.

Table 1. Morphometrics from UAV surveys

| Main Slump | | | | |
|--------------|---------------------|------|------------|---------|
| Date | A (m ²) | AAG% | Elongation | DTR (m) |
| 2016-09-28 | 1201 | | 1.82 | 106 |
| 2018-08-18 | 2608 | | 1.43 | 80 |
| 2019-05-19 | 3760 | 60 | 1.35 | 80 |
| 2019-09-25 | 4184 | | 1.37 | 66 |
| 2020-05-20 | 4228 | 32 | 1.37 | 66 |
| 2020-09-29 | 5519 | | 1.28 | 53 |
| 2021-05-06 | 5680 | 39 | 1.30 | 52 |
| 2021-11-03 | 7661 | | 1.14 | 36 |
| 2022-05-20 | 7783 | 19 | 1.14 | 36 |
| 2022-10-05 | 9091 | | 1.05 | 33 |
| 2023-05-18 | 9135 | 10 | 1.04 | 33 |
| 2023-09-07 | 10030 | | 1.00 | 32 |
| Second Slump | | | | |
| Date | A (m ²) | AAG% | Elongation | DTR (m) |
| 2021-10-07 | 394 | | 3.20 | 95 |
| 2021-11-03 | 414 | | 3.00 | 95 |
| 2022-05-20 | 424 | 88 | 3.00 | 95 |
| 2022-10-05 | 777 | | 2.53 | 80 |
| 2023-05-18 | 932 | 105 | 2.33 | 80 |
| 2023-09-07 | 1589 | | 1.82 | 69 |

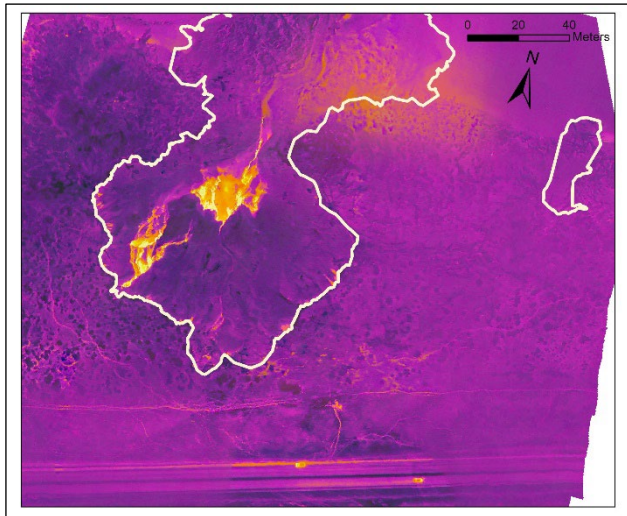


Figure 5. Aerial thermal imagery showing groundwater spring seeping from RTS 1 headwall.

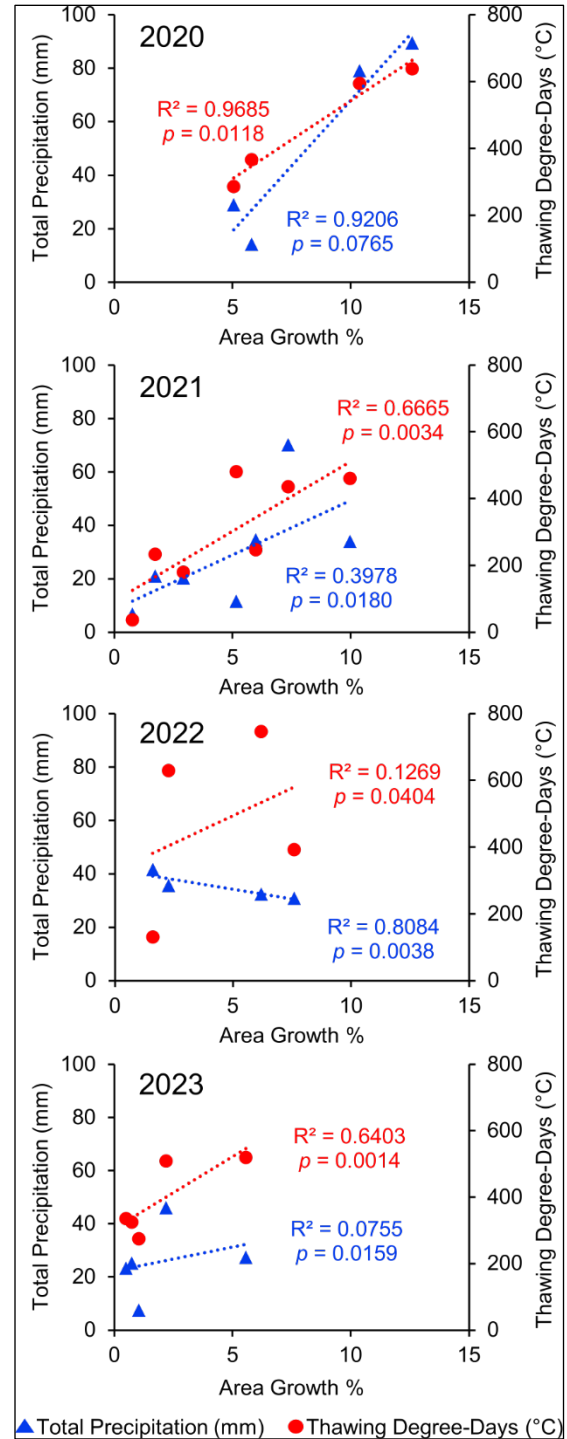


Figure 6. Surface area growth percentages vs. thaw degree-day value and the cumulative precipitation for the period between two summer UAV surveys.

5 DISCUSSION

5.1 Permafrost nature and origin

The geotechnical boreholes and ERT data show that permafrost at the RTS site formed in clayey silts which are frost susceptible. Permafrost temperature is warm, close to 0 °C. This area is consequently vulnerable to thaw. The ERT surveys showed thick, ice-rich permafrost in the forested area and more sporadic clusters of ice-rich permafrost closer to the road. This could be a result of decades of permafrost degradation under the right-of-way of the Alaska Highway since its construction in 1942.

The cryostratigraphical observations with the occurrence of suspended and thick layered cryostructure are consistent with syngenetic permafrost. The formation of this type of segregated ground ice generally occurs in fine-grained material, with abundant water supply, a slow thermal gradient, and usually an organic cover. Indeed, the abundant presence of deciduous trees and the absence of thick organic cover is atypical compared to other similar ice-rich epigenetic permafrost in discontinuous areas. Consequently, the permafrost on site may have originally formed under different environmental conditions, associated to a colder and more humid climate and different vegetation. The present-day warm permafrost temperature suggests that the relic permafrost is now in unstable equilibrium with the present climate.

This type of permafrost is generally associated with permafrost plateaus and frost heave mound environments (Calmels et al. 2008). Such conditions may have existed in the Takhini Valley when the permafrost developed. Although the vegetation and the topography have changed, the original cryostratigraphical imprint, shown by the ERT survey in the shape of ice-rich ground clusters, has remained unchanged. The shading provided by the newer deciduous forest may have contributed to the preservation of this relic permafrost.

5.2 RTS evolution

The progression of headwall and growth of the RTS 1 seem to decrease from one year to another, except for 2021. The rapid erosion of the headwall in 2021 could be related to extraordinary weather events that occurred during the summers of 2020 and 2021. Whitehorse had its ninth-rainiest summer in the weather records in 2020, with 157.8 mm over the course of the summer (Oakes 2020). Because of inertia in the system, the impact of this significant input of heat may have only been felt during summer 2021. In summer 2021 the “heat dome”, a mass of hot air sitting over the Pacific Northwest, occurred in June and July which resulted in warmer than average temperatures in the Yukon (Desmarais 2021), and could also have contributed to rapid erosion.

The decrease advance of the headwall at location of its central axis can be explained either by the lack of ground ice at this location to feed the process, or the compaction at that location by heavy machinery. The fact that the headwall section located only 10 m east of this disturbed area progressed by 14 m in summer 2022 and 13 m in summer

2023 suggests that the disturbance had an impact. The minimal progression at the west side during summer 2023 likely is attributable to the lack of ground ice in this undisturbed area. Ground ice content is variable at the study site, as shown by the ERT, and the slumping process is stalling at location where permafrost is ice-poor.

Analyses indicate that air temperature influences RTS thaw processes, while such influence was not proven for precipitation. These sites are impacted by rapidly occurring events such as heavy rain, heat waves, and unusually warm summer temperatures. Slump processes are preceded by pre-conditioning processes such as localized heat flow, ground water flow, thaw settlements, and deformation. A study by Ward et al. (2019) about RTSs in the Canadian High Arctic suggest that a decoupling of RTS dynamics from climate appears to occur over time for individual RTS as terrain factors take on a greater role controlling headwall retreat. This conclusion could also apply to the IbeX Valley RTSs. The complex interactions between those influencing factors require further analyses to better comprehend the development of RTSs. The on-going monitoring of RTS 2, that has been studied since its inception, might provide new insights in the future.

5.3 The role of groundwater

Geophysical and borehole data have emphasized the ice-rich nature of the ground at this site, as well as the presence of flowing ground water. While the thaw processes may have been initiated by bank erosion on the Takhini River, they have been exacerbated by the high ground ice content and the thermal effect of ground water flow. The UAV survey of the site using a thermal camera conducted in November 2021 has shown numerous ground water springs flowing in the slump and even generating icing events during winter. While it has not been quantified yet, ground water likely is contributing to permafrost degradation at this site.

6 CONCLUSIONS

The easy accessibility of the Takhini River site has enabled detailed and comprehensive investigation of retrogressive thaw slump processes in discontinuous permafrost. The multi-technical investigative approach highlighted permafrost features such as ground ice distribution, ground thermal regime, and groundwater flow. Frequent UAV surveys provided accurate morphometric measurements and a time-lapse evolution of two RTSs. They also provided the opportunity to investigate the relationship between the progression of the RTSs and climate at yearly and seasonal scales. Further research will allow for refinement of these studies and examination of the origin and impact of the groundwater flow on the RTSs.

Responding to the risk, the Yukon Department of Highways and Public Works has decided to relocate the road. The construction of a new section, about 80 m south of the current embankment, began in August 2023 and is scheduled to be completed during summer 2024. Because the current road and right-of-way has been degrading permafrost beneath it for decades, it is expected that, once abandoned, the old embankment will act as a barrier to the

headwall progression. Monitoring and investigations of the site will continue in the upcoming years.

7 ACKNOWLEDGEMENTS

The authors would like to acknowledge that the field sites are situated on the traditional territories of Kwanlin Dün First Nation and Ta'an Kwäch'än Council. We value the support of the Transportation Engineering Branch of Yukon Department of Highways and Public Works. We would also like to thank the numerous field and research assistants who made this work possible. Brian Horton and Stephie Saal from Climate Change Research at the YukonU Research Centre for the thermal imagery, Guy Doré and Chris Burn for their input. Thank you to the BMO Climate Institute for supporting and sharing our research.

Funding for this project was provided by Transport Canada's Northern Transportation Adaptation Initiative (NTAI) and National Trade Corridors Fund (NTCF). Additional funding was provided by ArcticNet, as well as by Crown-Indigenous Relations and Northern Affairs Canada's (CIRNAC) Climate Change Preparedness in the North (CCPN) program through the Government of Yukon's Department of Environment Climate Change Secretariat. In-kind contributions were also made by the Yukon Geological Survey, YukonU Research Centre, and Yukon government.

8 REFERENCES

Armstrong, L., Lacelle, D., Fraser, R., Kokelj, S., and Knudby, A. 2018. 'Thaw Slump Activity Measured Using Stationary Cameras in Time-Lapse and Structure From-Motion Photogrammetry', *Arctic Science* 4(4), pp. 827–845. doi:10.1139/as-2018-0016.

Ballantyne, C.K. 2018. *Periglacial Geomorphology*. New Jersey, United States: John, Wiley & Sons Ltd., ISBN 978-1-4051-0006-9.

Bernhard, P., Zwieback, S., and Hajnsek, I. 2021. 'Area and Volume Quantification of Arctic Thaw Slumps Using Time-Series of Digital Elevation Models', in *2021 IEEE International Geoscience and Remote Sensing Symposium IGARSS*. Brussels, Belgium: July 11–16, 2021, pp. 800–803. doi:10.1109/IGARSS47720.2021.9554503.

Burn, C.R. 1987. 'Thermokarst Ponds and Ground Temperatures In Takhini Valley', in S.R. Morison and C.A.S. Smith (eds.), *XII INQUA Congress, field excursions A20 and A20b Research in Yukon*. Ottawa, Ontario, Canada: July 31–August 9, 1987, p. 34.

Burn, C.R. 1998. 'The Response (1958–1997) of Permafrost and Near-Surface Ground Temperatures to Forest Fire, Takhini River Valley, Southern Yukon Territory', *Canadian Journal of Earth Sciences* 35, pp. 184–199. doi.org/10.1139/e97-10.

Calmels, F. Allard, M., and Delisle, G. 2008. 'Development and Decay of a Lithalsa in Northern Québec: A Geomorphological History', *Geomorphology* 97, pp. 287–299. doi.org/10.1016/j.geomorph.2007.08.013

Desmarais, A. 2021. 'N.W.T., Yukon break summer temperature records as heat dome lingers', *CBC News*, June 30, 2021. Available at: <https://www.cbc.ca/news/canada/north/temperature-highs-nwt-yukon-1.6085005>.

French, H.M. 2017. *The periglacial Environment*. 4th edition. Chichester, United Kingdom and Hoboken, New Jersey, United States: John Wiley & Sons. ISBN: 978-1-119-13278-3.

Hegginbottom, J.A., Dubreuil, M.A. and Harker, P.T. 1995. 'Canada, permafrost', in *National Atlas of Canada, 5th edition*. Natural Resources Canada, MCR 4177.

Kokelj, S.V. and Jorgenson, M.T. 2013. 'Advances in Thermokarst Research', *Permafrost and Periglacial Processes* 24(2), pp. 108–119. doi:10.1002/ppp.1779; ISSN 1099-1530. S2CID 140683397.

Kokelj, S.V., Kokoszka, J., van der Sluijs, J., Rudy, A.C.A., Tunnicliffe, J., Shakil, S., Tank, S., and Zolkos, S. 2021. 'Permafrost Thaw Couples Slopes with Downstream Systems and Effects Propagate Through Arctic Drainage Networks', *The Cryosphere* 15, pp. 3059–3081. Available at: <https://doi.org/10.5194/tc-15-3059-2021>.

Lewkowicz, A.G. and Way, R.G. 2019. 'Extremes of Summer Climate Trigger Thousands of Thermokarst Landslides In A High Arctic Environment', *Nature Communications* 10, 1329. Available at: <https://doi.org/10.1038/s41467-019-09314-7>

Oakes, B. 2020. 'The stats are in: It was a rainy summer in the North', *CBC News*, September 8, 2020. Available at: <https://www.cbc.ca/news/canada/north/rainy-summer-nwt-1.5713631>.

Ramage, J.L., Irrgang, A.M., Herzsich, U., Morgenstern, A., Couture, N., and Lantuit, H. 2017. 'Terrain Controls On The Occurrence of Coastal Retrogressive Thaw Slumps Along The Yukon Coast, Canada', *Journal of Geophysical Research: Earth Surface* 122(9), pp. 1619–1634. doi:10.1002/2017JF004231.

Turner, K.W., Pearce, M.D., and Hughes, D.D. 2021. 'Detailed Characterization and Monitoring of a Retrogressive Thaw Slump from Remotely Piloted Aircraft Systems and Identifying Associated Influence on Carbon and Nitrogen Export', *Remote Sensing* 13(2), 171. doi:10.3390/rs13020171.

van der Sluijs, J., Kokelj, S.V., Fraser, R.H., Tunnicliffe, J., and Lacelle, D. 2018. 'Permafrost Terrain Dynamics and Infrastructure Impacts Revealed by UAV Photogrammetry and Thermal Imaging', *Remote Sensing*, 10(11), 1734. doi.org/10.3390/rs10111734.

Ward Jones, M.K., Pollard, W.H., and Jones, B.M. 2019. 'Rapid Initialization of Retrogressive Thaw Slumps In The Canadian High Arctic And Their Response To Climate And Terrain Factors', *Environmental Research Letters* 14(5), 055006. doi:10.1088/1748-9326/ab12fd

Yukon Ecoregions Working Group 2004. *Ecoregions of the Yukon Territory: Biophysical Properties of Yukon Landscapes*, C.A.S. Smith, J.C. Meikle and C.F. Roots (eds.). Summerland, British Columbia, Canada: Agriculture and Agri-Food Canada, PARC Technical Bulletin No. 04-01.